Surgical Idiosyncrasies Credentials using Image Registration

by G. Tirumala Vasu, Samreen Fiza

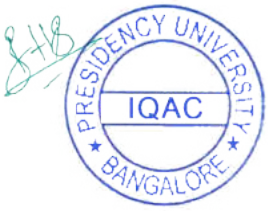

Submission date: 07-Mar-2022 03:12PM (UTC+0530)
Submission ID: 1778432760
File name: urgical_idiosyncrasies_credentials_using_image_registration.docx (1.23M)
Word count: 6022
Character count: 34242

Surgical Idiosyncrasies Credentials using Image Registration

G. Tirumala Vasu[1], Samreen Fiza[2], G Swetha[3], Hari Banda[4]
[1, 2, 3]*Department of Electronics and Communication Engineering, Presidency University, Bangalore, India.*
[4] *Department of Mechanical Engineering, Villa College, Maldives.*
[1]*tirumala.vasu@presidencyuniversity.in*, [2]*samreenfiza@presidencyuniversity.in*,
[3]*swethag@presidencyuniversity.in*, [4]*banda.hari@villacollege.edu.mv*

Corresponding author 1: Hari Banda, *banda.hari@villacollege.edu.mv*
Corresponding author 2: G. Tirumala Vasu, *tirumala.vasu@presidencyuniversity.in*

Abstract

In standard image registration, the point of interest deals with the detection and selection of feature points. In addition to this, we introduce the motion vectors for detecting the specific object deviation by setting the threshold level. Block matching motion estimation algorithm is used in identifying the translational movement which is an essential measure in medical imaging, particularly to detect abnormalities related to loosening, subsidence and anteversion. Convolutional filters are more effective in searching the key points. Hessian differential operators, octave and level sampling are used for filtering the features. For selecting feature points, interpolation parameters and nonmaximum dominance of differential operators are used.

Keywords
Differential Operators, Feature Point Detection, Feature Point Selection, Motion Estimation, Motion Vectors, Block Matching Motion Estimation.

I. INTRODUCTION

Inside the current medical setting, clinical imaging is an imperative segment of countless applications. Such applications happen all through the clinical track of the occasion, not just inside demonstrative settings, however, unmistakably in the zones of arranging, completing and assessing careful and radio therapeutic approaches. The imaging modalities used can be partitioned into anatomical and functional classes. The Anatomical modalities, for example, portraying morphology, incorporate X-ray or X-beam, MRI (Magnetic Resonance Imaging), CT (Computed or figured tomography), US (Ultrasound), entry pictures and video arrangements acquired by different catheter 'scopes', for example in laparoscopy some noticeable subordinate strategies are so disengaged from the first modalities that they show up under a different name, for example MRA (Magnetic Resonance Angiography), DSA (Digital Subtraction Angiography, got from x-ray), CTA (Computed Tomography Angiography) and Doppler (got from US, alluding to the Doppler impact estimated). Functional modalities, i.e. depicting fundamentally data on the digestion of hidden life structures, incorporate (planar) scintigraphy. SPECT (single-photon emission computed tomography), PET (Positron emission tomography), which together make up the atomic medication imaging modalities and fmRI (functional MRI). With a little creative mind, spatially meager systems like EEG and MEG can likewise be called utilitarian imaging systems. A lot of progressively utilitarian modalities can be termed, however these are either minimally utilized, or still in the preclinical research arrangement, e.g., pMRI (perfusion MRI), EIT (electrical impedance tomography).

Since the data picked up from two pictures gained in the clinical track of occasions is for the most part of a correlative nature, proper reconciliation of helpful information obtained from the different pictures is regularly wanted. The initial phase right now is to bring the modalities required into a spatial arrangement, a methodology alluded to as enrollment. After enrollment, a combination step is required for the coordinated presentation of the information in question. Lamentably, the terms enrollment and combination, just as coordinating, joining, connection and others, show up polysemous in writing, either alluding to a solitary advance or to the entire of the methodology incorporation process. Right now, the meanings of enrollment and combination as characterized above will be utilized.

The picture enlistment is one of the key strides to accomplish three-dimensional (3D) limitation and the other picture combination forms [16]. The strategies for picture enrollment are mostly named enlistment based on dark enrollment in change space and the enrollment techniques dependent on highlights. Enrollment technique dependent on dim does the geometric change of the picture to be enrolled and afterward picks the fitting advancement calculation to acquire the enrollment change framework. Its estimation is basic. Be that as it may, it requires high picture quality and is anything but difficult to be influenced by outer conditions [1], [2], [3], [4], [5], [9]. Enrollment technique dependent on change area utilizes a sort change to acquire the interpretation, revolution, scaling, and other parameters between pictures. The Fourier change is generally utilized. This sort of strategy has a better enemy of commotion, also the quicker speed. In any case, it is primarily reasonable for the basic twisting between pictures [6], [9].

Picture enlistment is a way of adjusting pictures obtained from various imaging frameworks [7], [8] by finding the right spatial change between related components in pictures. Enrollment of pictures gained from various sensors or on the other hand imaging conventions has various clinical applications in finding and picture guided medical procedures/ treatments [10]. The test is to manage a large range of force varieties beginning from enlightenment changes, in-homogeneity, or essentially imaging modalities. Since various physical wonders are estimated in various imaging frameworks, no practical connection between the picture powers can be characterized to delineate the relating components starting with one picture then to the next. With the advancement of remote detecting innovation, multitemporal, multispectral, and multiresolution remote detecting information have risen. These information give correlative data for the investigation of the quality of the locale and a total portrayal of the highlights [11]. Picture enrollment innovation is essential for the extensive utilization of this picture data [12]. Picture enrollment is of vital significance in incorporating data from pictures of a similar zone of intrigue that are gathered from various estimations [13], [14], [15], either at various time space, or utilizing an alternate methodology. For instance, in remote detecting, skillet honing is a system to intertwine a high spatial goals panchromatic pictures with low spatial goals, RGB or multi-ghastly pictures. To accomplish high spatial and ghastly goals pictures, an exact enlistment between the PAN and the multi-ghastly pictures is required.

II. DIFFERENTIAL OPERATORS FOR KEY POINTS

In image processing, detecting the features of an image plays an important role. This process is useful to identify the objects in an image and compare the same objects in another image. In many medical image processing techniques [21], which involves feature detection, by means of extracting the features of a particular image automatically with the unique content of the object. This process was used to identify different objects from the image. Generally, the process of identifying the objects in an image is possible, if the reference image is focused using transformations like shifting with some scale or otherwise rotating with some angle.

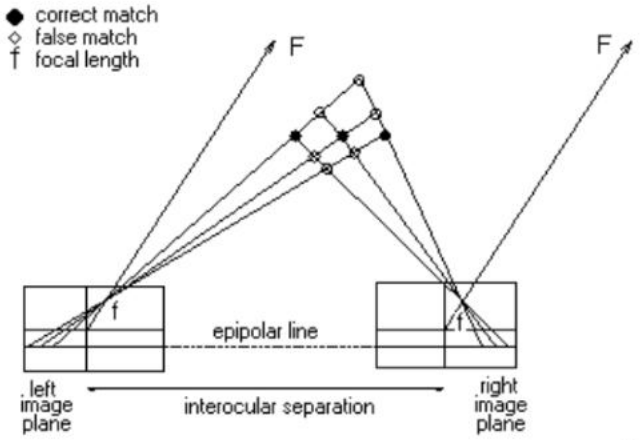

Fig. 2.1: Correspondence between the two images

In many computer vision applications the above said process was used. Registering the feature points of an image, object recognition and object tracing are examples of computer vision. To know what exactly the correspondence between the images, just observe the diagram Fig. 2.1. Few points from the left image plane are matched with the right image plane. In an image, the correspondence between the pixels can be

calculated in so many ways, but among them the following three steps are mainly used, the foremost one is interest points selection from different locations in an image like corners, globules and intersections. The second step is finding the feature vector from the neighborhood pixels of every point of interest from different observing conditions [19]. Final step is accomplishing all pixels as a descriptor vector that are coordinated between different images. This type of matching was performed by calculating the distance between the vectors. Using general geometrical calculations like Euclidean distance, the correspondence can be calculated.

A. Convolution filters

One of the linear filters that were used in the spatial domain and the simplest among all other filters are box -filters. It replaces a pixel in an image with its average value of neighborhood pixels [25], and this is a simple average method performed on pixels. Box-filters are used to find the average value of neighborhood 4-connectivity or 8- connectivity pixels as shown in figure 2.2.

The main benefit of this type of average filter is to decrease the irrelevant data from the image. Use of this special box-filter confines the problem to its coefficients, i.e., all coefficients are equal. To overcome this confliction, convolution filters are used where we can observe different useful coefficients in the image. Convolution filters are also used in smoothing, sharpening, intensify and enhance the image. If we are dealing with medical images, the enhancement process is very useful. Thus, in this proposed method, the use of box-filters in Speeded-up Robust Feature (SURF) algorithm was modified with a convolution filter.

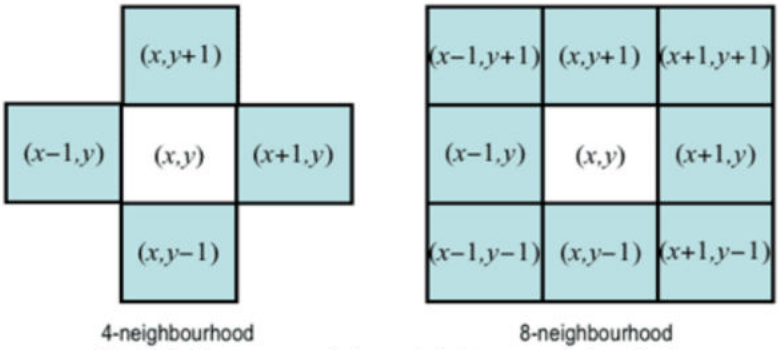

Fig. 2.2: Four connectivity and eight connectivity pixels

Convolution filters working with masks of size 3*3 or 9*9 sometimes are called convolution symmetric kernels [26]. Let the coordinates of the image be (x,y) and 'L' be the scale parameter which can characterize the size of filter. The general property of the convolution filter is given below.

$$\forall (x,y) \in Z^2, (f * g)(x,y) := \sum_{(i,j)\in\Omega} f(x-i, y-j)\, g(i,j) \tag{2.1}$$

Discrete differential operators are used in convolution filters with several scales which are used to improve the filter efficiency and perform parameterized operation with suitable kernel by above mentioned variable 'L'. To do this operation, first-order and second-order convolution filters are used.

B. First order convolution filter

Let us consider a digital image 'u' and this can be operated with the true values of the operator at a scale 'L' accomplished with prime coordinate referred to as 'D' multiplied with x*L. It creates the convolution filter with suitable size

$$\ell(L)=\lceil 0.8L \rceil \in \boldsymbol{N} \tag{2.2}$$

Recollecting the information where the symbol [.] represents the round off operation to the next higher value of integer.

$$D_x^L u := (B_{[-l,-1]^x[-l,l]} - B_{[1,l]^x[-l,l]}) * u$$

$$D_y^L u := (B_{[-l,l]^x[-l,-1]} - B_{[-l,l]^x[1,l]}) * u \tag{2.3}$$

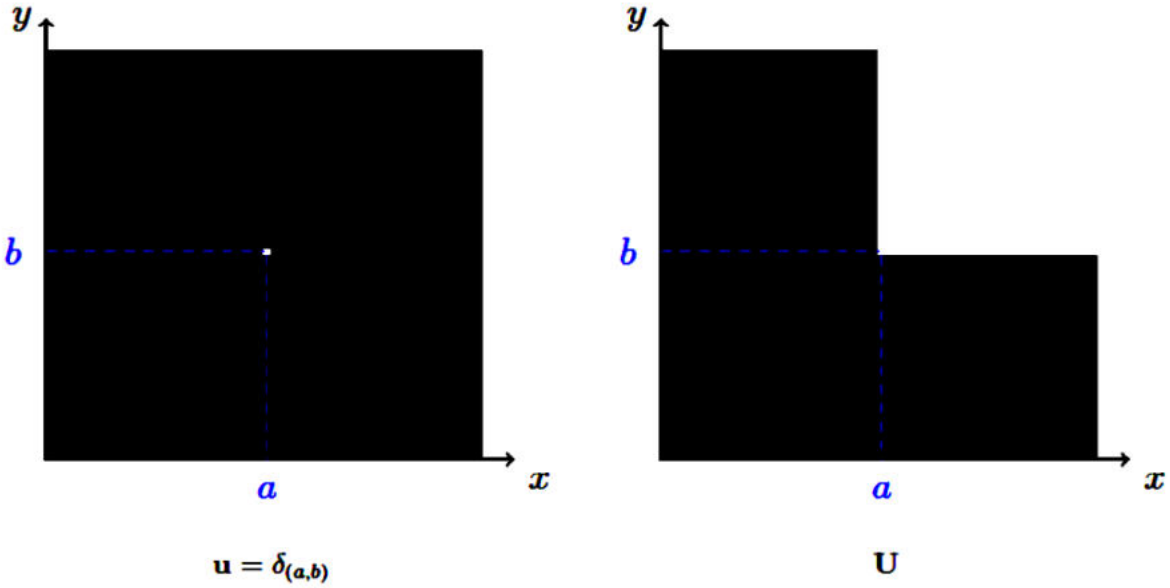

Fig. 2.3: Left side image consists of a test image 'u' and the right side image consists of its integral 'U'

In the above image 'u' consists of a single nonzero pixel. We can identify that, if ℓ= 1, the convolution filter performs the operation as a symmetric finite-difference mechanism at the pixel range of scale.

$$u = \begin{bmatrix}1\\1\\1\end{bmatrix}^x [1\ \ 0\ -1] * u = \begin{bmatrix}1 & 0 & -1\\1 & 0 & -1\\1 & 0 & -1\end{bmatrix} * u \tag{2.4}$$

The above explained filters are first-order convolution filters. These filters use first-order partial derivatives as operators in a preference scale ℓ. We can get a good suitable formula for its impulse of 'D' multiplied with xL operator.

$$D_y^L \delta(x,y) = \begin{cases} 1 & if(x,y) \in [-l,l]^x[-l,-1] \\ -1 & if(x,y) \in [-l,l]^x[1,l] \\ 0 & otherwise \end{cases} \tag{2.5}$$

Computational complexity calculation using the integrated image as explained in equation (2.2) we can pre determine the integrated image say 'U', seven consecutive additions are enough to evaluate those operators irrespective of size of the parameter ℓ. Now let us consider and evaluate [29] the same equation (2.2) with 'b' and 'a' equal to ℓ and c = -ℓ, d = -1.

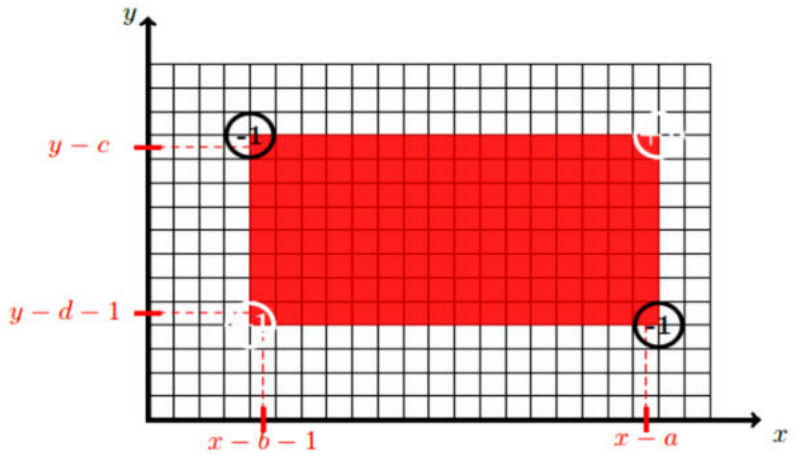

Fig. 2.4: Operation of convolution filter using integral image

We can get,

$$\forall (x,y) \in \Omega,\ D_y^l u(x,y) = \begin{aligned} & U(x+l, y+l) + U(x-l-1, y) \\ & -U(x+l, y) - U(x-l-1, y+l) \\ & -U(x+l, y-1) - U(x-l-1, y-l-1) \\ & +U(x+l, y-l-1) + U(x-l-1, y-1) \end{aligned} \tag{2.6}$$

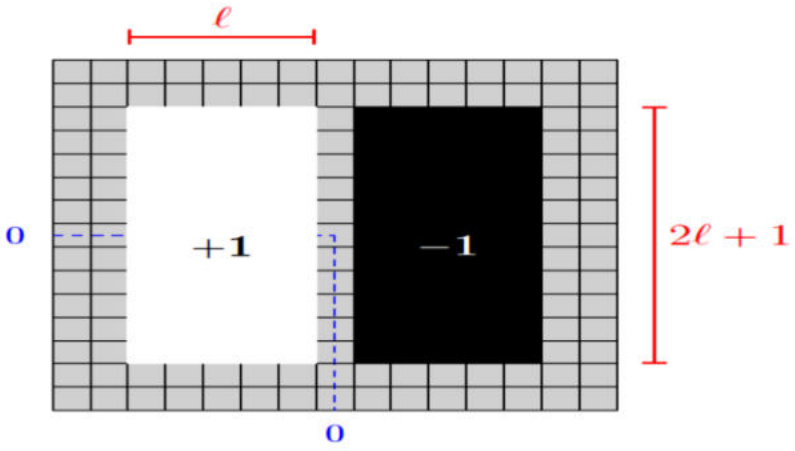

Fig. 2.5: Overview of first-order convolution filter

III. PROPOSED METHOD

As shown in Fig. 3.1, the proposed surgical idiosyncrasies credentials using image registration approach majorly consists of five steps:

1) Calculating differential operators for two reference images
2) Key points detection which involves Hessian matrix determinants, octave sampling and level sampling
3) Key points selection based on the detected features of step 2
4) Matching the key points of two reference images
5) Calculating the motion vectors for identifying the deviation

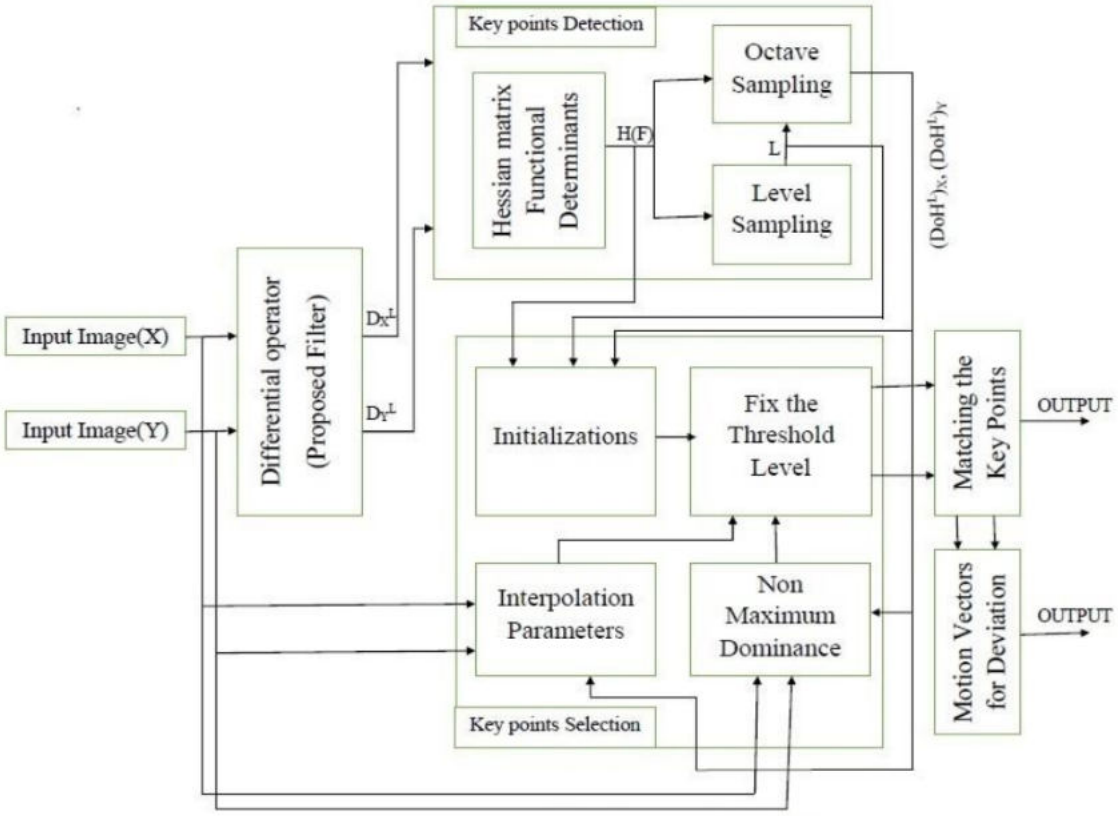

Fig. 3.1: Schematic of Proposed Method

Two reference images, say X and Y, are considered. Differential operators will be calculated separately for both reference images by using the above said convolutional filter equation 2.3.

A. Key Points Detection

In the above section, the structures of first-order and second-order convolution filters and how these filters are configured with its parameters were explained. In this section, we will find key points through multiscale adaptive local feature detection. The term 'multiscale' is introduced here because the convolution filter [28] produces the response with scale invariant property, i.e., the filter response should not vary with its operator's scale. Algorithm follows the steps shown below. Here, the input is taken as 'u' and it produces a list of key points from the reference image.

Step-1: Initialization of two reference images like U_x and U_y
Step-2: For loop starts with L=1 to 2
Calculating Hessian matrix
End For loop
Step-3: Select key points with some modification
Step-4: For loop starts here to perform Octave Sampling
For loop starts here to perform Level Sampling
Calculate 2^{oi} and produce L
List key points by adding to Hessian matrix coefficients
End for loop
End for loop

Step-5: Return all key points

By using the above algorithm, we can detect feature points and some important terms related to this algorithm like Hessian matrix coefficients, active samplers as explained below.

B. Filtering of Features

Second order partial derivatives are arranged in a square matrix as shown below, which forms Hessian matrix or simply Hessian. Usually Hessian matrix uses the functional determinants.

$$\mathbf{H(F)}=\begin{bmatrix} \frac{\partial^2 f}{\partial x_1^2} & \frac{\partial^2 f}{\partial x_1 \partial x_2} \cdots & \frac{\partial^2 f}{\partial x_1 \partial x_n} \\ \frac{\partial^2 f}{\partial x_2 \partial x_1} & \frac{\partial^2 f}{\partial x_2^2} \cdots & \frac{\partial^2 f}{\partial x_2 \partial x_n} \\ \vdots & \vdots \ddots & \vdots \\ \frac{\partial^2 f}{\partial x_n \partial x_1} & \frac{\partial^2 f}{\partial x_n \partial x_2} & \frac{\partial^2 f}{\partial x_n^2} \end{bmatrix}$$

Fig. 3.2: Hessian matrix of order n

Hessian determinant calculation using convolution filters: The scale-independent Hessian matrix determinants can be calculated from the below equation.

$$\mathrm{D_oH^L(u)}:=\frac{1}{L^4}\left(D_{xx}^{L}u.D_{yy}^{L}u-(w\,D_{xy}^{L}u)^2\right) \tag{3.1}$$

As we mentioned in the above algorithm, scaling can be achieved from the relation $L=2^o i+1$ and here the constant predefined weight 'w' is 0.912. Normalization factors are required to get the scale invariance property, generally we will take $\frac{1}{L^4}$ as a normalization factor. While calculating the Hessian determinant, the numerical tolerance will come into picture to overcome this weighting factor 'w' which was used. Each point of the box space, almost 36 operations are required for computation of this operator and this process can perform to compute $\mathrm{DoH^L(u)}$, which is clearly explained in the below algorithm.

The matrix parameters multiplied [17] with every pixel in an image leads to an increase in the computational complexity [29]. To reduce the computational complexity while calculating the Hessian determinant, sampling is required. The sampling is performed in the octal level so that the number of pixels to be tested is $[\frac{M}{2^{o-1}}]$ X $[\frac{N}{2^{o-1}}]$. After finding Hessian determinants using convolution filters, it is necessary to normalize the determinants because those values are continuous and the convolution filters are not isotropic. As mentioned above, to realize the scale invariance, the Hessian operators has to normalize and we can get ℓ^2 constants from the entire scale. The same is given below

$$\|D_{xx}G_\sigma\|_2^2=\frac{3}{16\pi\sigma^6}=3\|D_{xy}G_\sigma\|_2^2 \tag{3.2}$$

The algorithm given below shows how to detect features from the Hessian determinants. Here the input arguments are image integrated image (U), Octave sampler (o), Level labelled as 'i' and the output is '$\mathrm{DoH^{L'}}$.

Step-1: Initialization of Hessian determinants
Step-2: Calculate 2oi+1 as L
Step-3: For loop start with 0 to M-1
    Perform 2o-1 Correspondence
    For loop start with 0 to N-1
        Perform 2o-1 Correspondence
        Use 3.1, Calculate Hessian scale independent values

End for loop
End for loop
Step-4: Return $(DoH^L)_x$, $(DoH^L)_y$

C. Selection of Key Points

After detecting the feature points, we have to select only a few of them which are adaptively considered matched with the reference image, this can be achieved by considering the neighborhood pixels. In this selection, the class of transformation which we used at the time of feature detection procedure was important. By considering similarity parameters like location and shape, scale estimation is jointly performed with similarity transformation.

In this methodology, the common interest or desirable points are considered as the local maxima of the determinants of Hessian matrix (DoH^L) of an image (u). Now, the detection of maxima is performed [22] by considering P, Q, R neighborhood pixels, generally P=Q=R=3, and comparing the box space with the nearest neighborhood pixels. The above said procedure is described in the below algorithm.

This algorithm consists of input arguments which are maxima of the determinants of Hessian matrix (DoH^L) of an image (u), octave sampling(o), Level of interest (i), DoH^L values at 'o' and 'i'. Then the output arguments are a list of key points.

Step-1: Initialization of Octave Sampler, Level of interest and Hessian determinants
Step-2: Calculate 2oi+1 as L
Step-3: For loop start with 0 to M-1
Perform 2o-1 Correspondence
For loop start with 0 to N-1
Perform 2o-1 Correspondence
Use equation 3.3 to fix the threshold
Maximum dominance calculation for $(DoH^L)_{X,Y}$
Interpolation parameters Calculation for $(DoH^L)_{X,Y}$
End for loop
End for loop
Step-4: Return the list of key points

Procedure to set the threshold: Thresholding is essential process after quantization with octaves. Here we are using four number of octaves and two number of levels for analysis so that we can analyze 8 scales of representation. Using the method as in [25] is not only a computationally efficient method of image representation but also provides noise immunity. We can get the key features by applying a threshold on Hessian determinants (DoH^L).

$$DoH^L(image)(x,y) > L \tag{3.3}$$

We have to remember that this operator is scale invariant and it is constant. This normalization can be achieved using simple mathematical operations. By using trial and error method also we can set the threshold [27], let the threshold value be 103 and the reference image interval be [0,255]. Fig. 3.3 describes setting the points of interest with reference to Hessian determinants (DoH^L) after the thresholding operation. The radii of the green circles is variable, in this application the radii is set to 2.5 times the L (Box Scale).

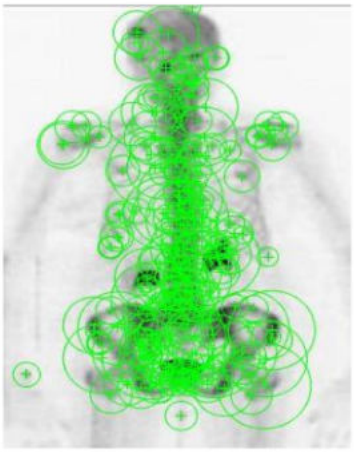

Fig. 3.3: Illustration of interest point detection

As stated above, for scale normalization, Hessian determinants are used. However, we may use a few other operators like Laplacian. The mathematical formulation of Laplacian operator is as given below.

$$\Delta^L(u) := \frac{1}{L^2}(D^L_{xx} + D^L_{yy})u. \tag{3.4}$$

D. Matching the Key Points

After selecting the key points from two images, say 'u' and 'v', match the key points which are represented by its point of interest ($\{X_k\}_k$ and $\{Y_\ell\}_\ell$) with their corresponding descriptors (SURF of $\{X_k\}_k$ and SURF of $\{Y_\ell\}_\ell$). We know that, for this type of descriptor, the interest points must satisfy the condition X $\epsilon[-1,1]^{64}$ which indicates a vector with dimension 64 and its Euclidean norm is $\| X \| = 1$. The comparison between the interest points was performed using Euclidean distance, since these interest points are considered as vectors. After that, using a thresholding technique called Nearest-Neighbour Distance Ratio (NNDR), we can combine the features. Here, we calculate the Euclidean distance by comparing the descriptor X_k with the image 'u'.

$$d^2_{k,l} = \|X_k - Y_l\|^2_2 = 2(1 - X^T_k . Y_l) \tag{3.5}$$

Let us consider one megapixel image, almost millions of scalar products are computed from the second image 'v', this extends the computational complexity. Therefore, to lessen the computational complexity in the matching procedure, we need to compare the Laplacian signs of key features. If the two descriptor's signs are not equal, then those are considered as unlikely similar. In this case, there is no need to compare the key features and the comparison is discarded.

For matching the key points we need to find the most important and reliable correspondence from several number of reputed features, this leads to best match of feature. In the other way, if we consider the similarity distance sd_k only into account, it is necessary to separate the true match from the false match. Using the nearest neighbour matching method may or may not produce the best match because it considers only correspondence between X_k and its most similar one, denoted by '$Y_{\ell 1}$' where $\ell 1$ is,

$$l_1 \in arg^{min}_l \, d_{k,l} \tag{3.6}$$

The Nearest Neighbour Distance Threshold is a proximity search technique which is used in pattern recognition, computer vision, etc., this is a straightforward method to find the correspondence by fixing threshold on the similarity measure. Indeed, such a method of matching produces a negotiation between false positive numbers and false negative numbers. Therefore instead of using this type of thresholding method [19], we used Nearest Neighbour Distance ratio, which is a simple and reliable statistical method to discard mismatches.

In this method of matching, we need to find the ratio of the first and second nearest neighbour pixels and measure the correspondence between them. For doing this, first we have to compute Y_{l1} and then other closet one Y_{l1}features from the desired X_k,such that

$$l_2 \in arg^{min}_{l,s.t.\ d_{k,l} \geq d_{k,l_1}} d_{k,l} \tag{3.7}$$

Finally, compare the corresponding ratio to a suitable threshold 't' and follow the condition, if $\frac{d_{k,\ell_1}}{d_{k,\ell_2}} \leq$ t, then the correspondence was confirmed in this discussion, and the threshold was set to t=0.8, we may increase or decrease the threshold using trial and error methods. We are dealing with medical images so that the threshold was set to maximum value. After the matching is completed, it is necessary to find the deviation of the matched points. This is explained in the below section.

E. Motion Vectors to Find Deviation

This Unit describes the motion estimation theory between two consecutive images using features. The key idea of motion estimation is to find [17] the displacement between two successive frames. In the simplest form, the problem can be described by equation (3.8). This equation only permits the registration of translational movement in x and y and the intensity levels are expected to be the same all over the image.

$$I(x, y, t) = I(x + \Delta x, y + \Delta y, t - \Delta t) \tag{3.8}$$

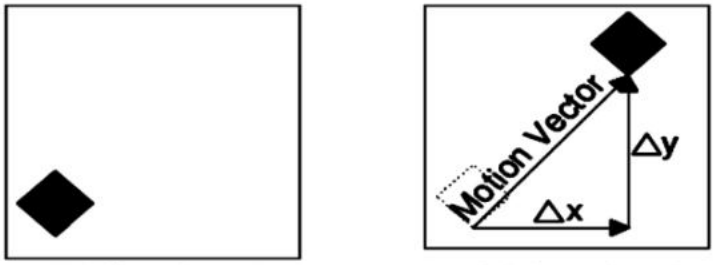

(a) Reference image 1 (b) Reference image 2

Fig. 3.4: Displacement between frames

Frame Translation: The general model of inconsistency between two objects in two respective frames is translation. Translation can identify the movement of any particular region in an image. Naturally, if an image is affected by translational movement, then it indicates objects [18] in the foreground have been moved. Suppose the translational movement is outside the reference image, then the new frame is created by the combination of both old coordinates plus translation coefficients.

$$\begin{bmatrix} x_{new} \\ y_{new} \end{bmatrix} = \begin{bmatrix} x_{old} \\ y_{old} \end{bmatrix} + \begin{bmatrix} \Delta x \\ \Delta y \end{bmatrix} \tag{3.9}$$

In the above equation, X_{old}, Y_{old} are the old coordinates of the image in which the translation operation was performed. X_{new}, Y_{new} are the new coordinates after performing the translation operation. The numerical values Δx and Δy are the small translational movement in X-axis and Y-axis direction, respectively. Each pixel of the frame was translated and new coordinates were obtained from equation 3.9. Here, we have to remember that the entire frame was modified with new coordinates and the frame was neither damaged nor corrupted by noise. In the translation operation [22], all pixels of the original image are imposed in the output image, the region of interest was moved to the desired position [19, 20] using equation 3.9. If all pixels of original image are left unchanged, then the translated image is the same as the original image which means that there is no change in the output image. We can observe a slight difference

between moving the pixel region and translating the pixel region, if original pixel region was filled with homogenous gray levels. An example of translation operation is given below Fig. 3.5.

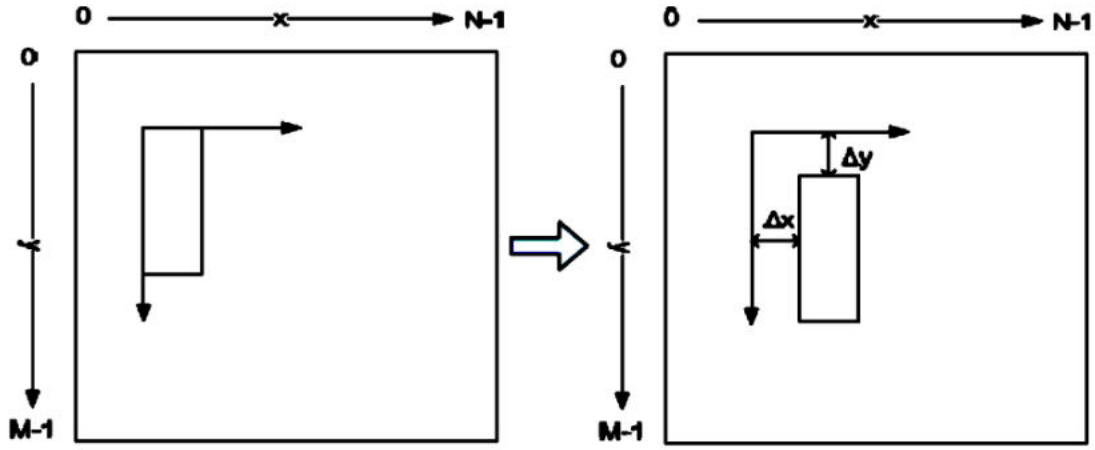

Fig. 3.5: Example for Translational operation

Since the pixel values of an image are integers, the translation procedure is straight forward and if we use sub-pixel values, we may use the bilinear interpolation method.

Rotation of an image: Spatial transformation techniques have a vital role in many image processing applications like CT, MRI images. Rotational operation is one of the linear spatial transformation methods [23]. This type of operation was characterized by center of rotation and rotational angle.

Let us consider the camera movement to be anti-clockwise rotation. Then the entire frame will be a clockwise rotation of all pixel values to a new location.

$$\begin{bmatrix} x_{new} \\ y_{new} \end{bmatrix} = \begin{bmatrix} cos\theta & -sin\theta \\ sin\theta & cos\theta \end{bmatrix} \begin{bmatrix} x_{old} \\ y_{old} \end{bmatrix} \tag{3.10}$$

Here in the equation, θ represents the rotational angle. For more reliable analysis it will be indicated like

$$\begin{bmatrix} \bar{x}_{new} \\ \bar{y}_{new} \end{bmatrix} = \begin{bmatrix} cos\theta & -sin\theta \\ sin\theta & cos\theta \end{bmatrix} \begin{bmatrix} \bar{x}_{old} \\ \bar{y}_{old} \end{bmatrix} \tag{3.11}$$

Here the quantity $\bar{x}$ measures the average value, equation 3.11 is rewritten as in equation 3.12,

$$\begin{bmatrix} x_{new} - \bar{x}_{new} \\ y_{new} - \bar{y}_{new} \end{bmatrix} = \begin{bmatrix} cos\theta & -sin\theta \\ sin\theta & cos\theta \end{bmatrix} \begin{bmatrix} x_{old} - \bar{x}_{old} \\ y_{old} - \bar{y}_{old} \end{bmatrix} \tag{3.12}$$

In numerous case, and more desirable cases involving medical applications [24], analyzing the rotational movement of individual objects in the frame is needed. Equation 3.10 enables such type of mechanism. As mentioned in the above equations, we conclude the new coordinates for the rotated image will be as given in equation 3.13

$$\begin{bmatrix} x_{new} \\ y_{new} \end{bmatrix} = \begin{bmatrix} cos\theta & -sin\theta \\ sin\theta & cos\theta \end{bmatrix} \begin{bmatrix} x_{old} - \bar{x}_{old} \\ y_{old} - \bar{y}_{old} \end{bmatrix} + \begin{bmatrix} \bar{x}_{new} - \bar{x}_{old} \\ \bar{y}_{new} - \bar{y}_{old} \end{bmatrix} \tag{3.13}$$

IV. RESULT ANALYSIS

In this section, we used six test samples of medical images. The experiment with the proposed method of image registration not only performed feature detection but also identified how much the specific object was deviated from the reference image before and after surgery. In fig. 4.1, (a) and (b) are two reference images of bone surgery. From equations (3.3) and (3.4), the strongest key points are selected as shown in fig. 4.1 (c), (d), (l) and (m). Here we can identify clearly that there was no deviation in the objects. The same statement can be justified by quantitative values of fig. 4.1 (g), (h) and (i). The linearity in the curve of fig. 4.1 (g), (h) and (i) shows that there is no deviation, but this linearity in the slope is not observed in fig. 4.1 (r) which indicates a small deviation. In fig. 4.1 (e) slope of the matched features is zero and fig. 4.1 (n) has some slope. The motion vector analysis performed on the test sample further justifies the proposed algorithm. If we compare fig. 4.1 (f) and (o), in the former there are no motion vectors because there is no deviation, but in the latter we can observe a few motion vectors.

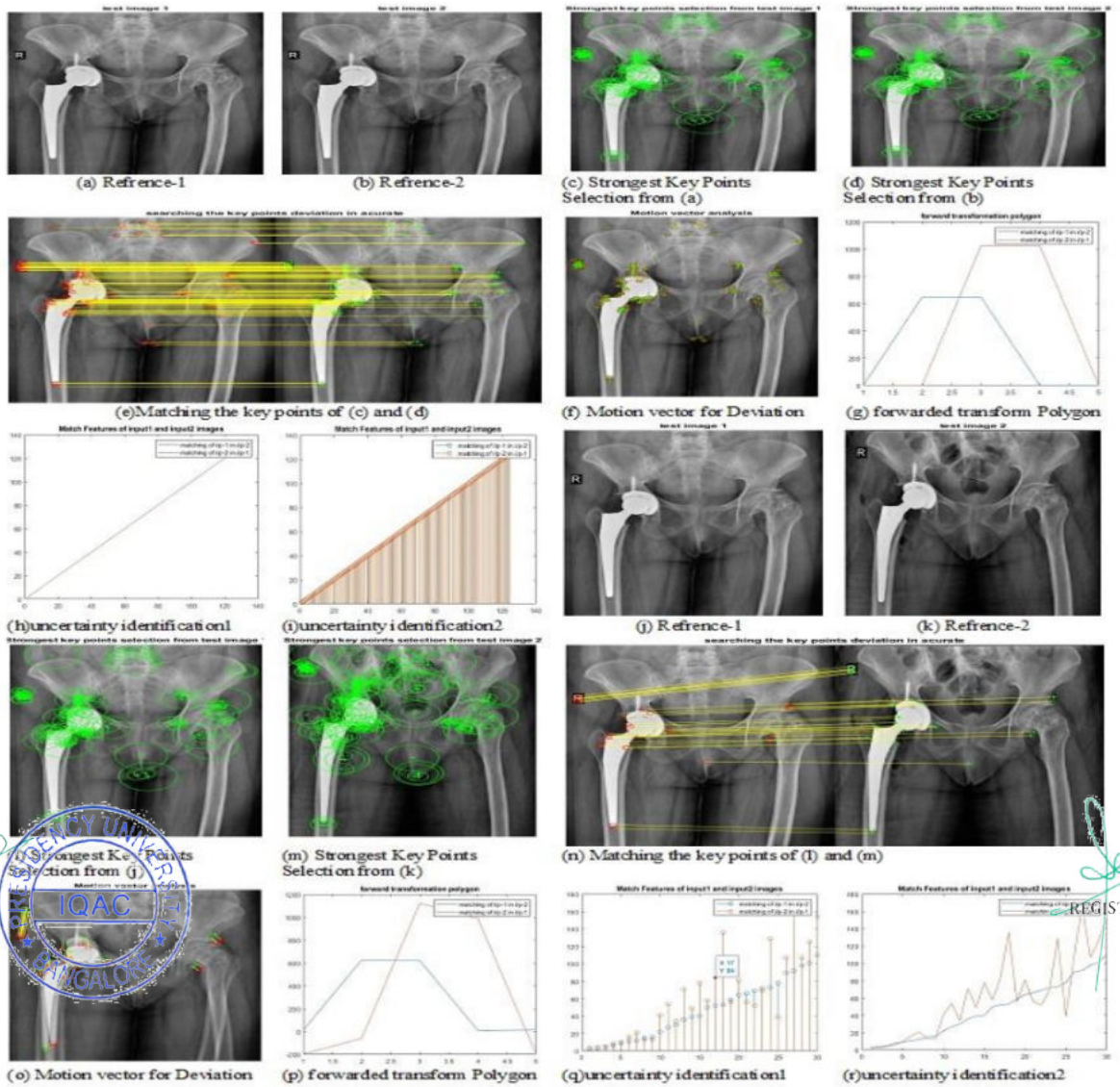

Fig 4.1: (a-i) Hip replacement surgery without deviation, (j- r) Hip replacement surgery with deviation

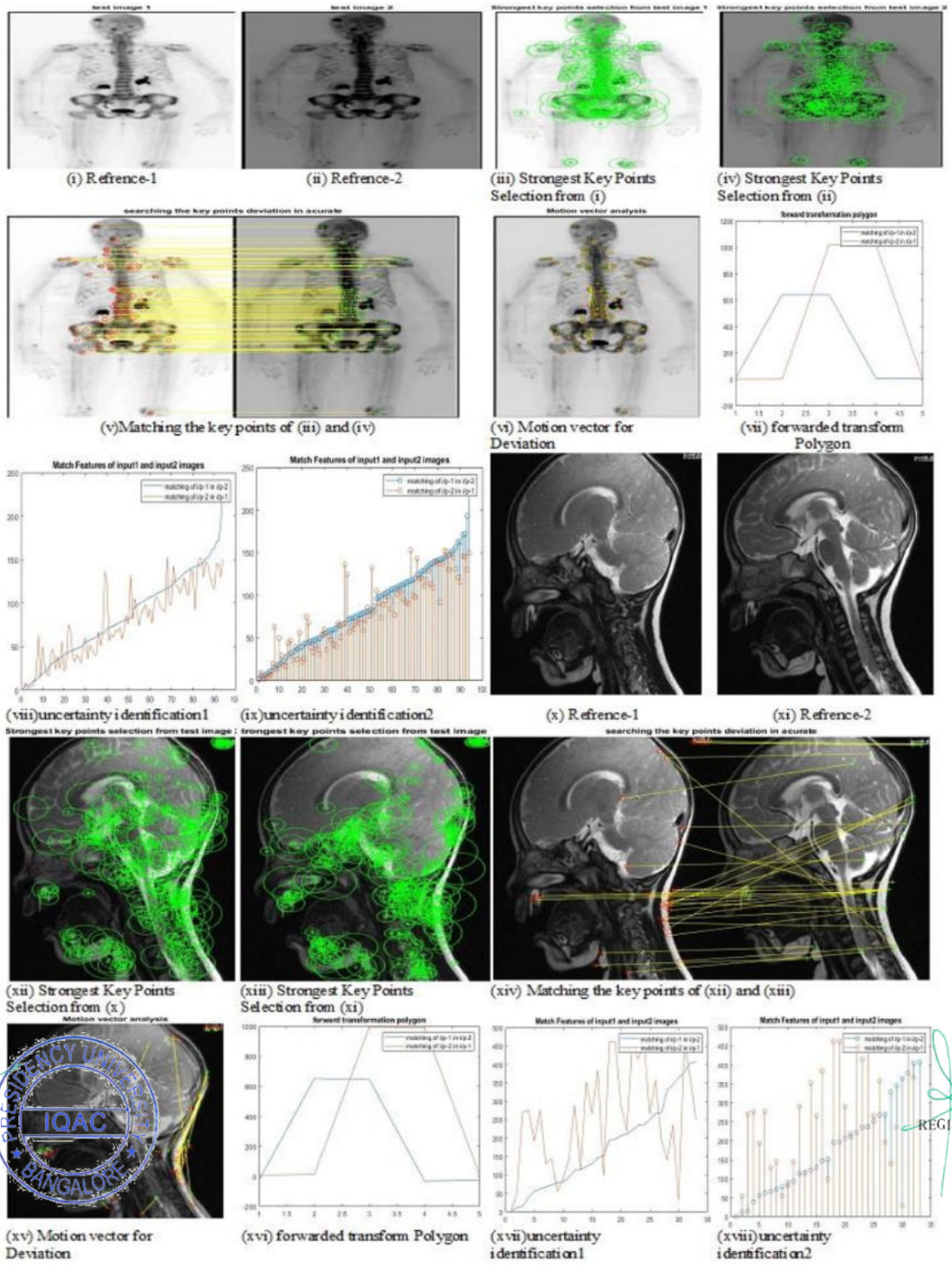

Fig 4.2: (i-ix) Backbone surgery sample without a deviation, (x-xviii) Brain sample with a deviation

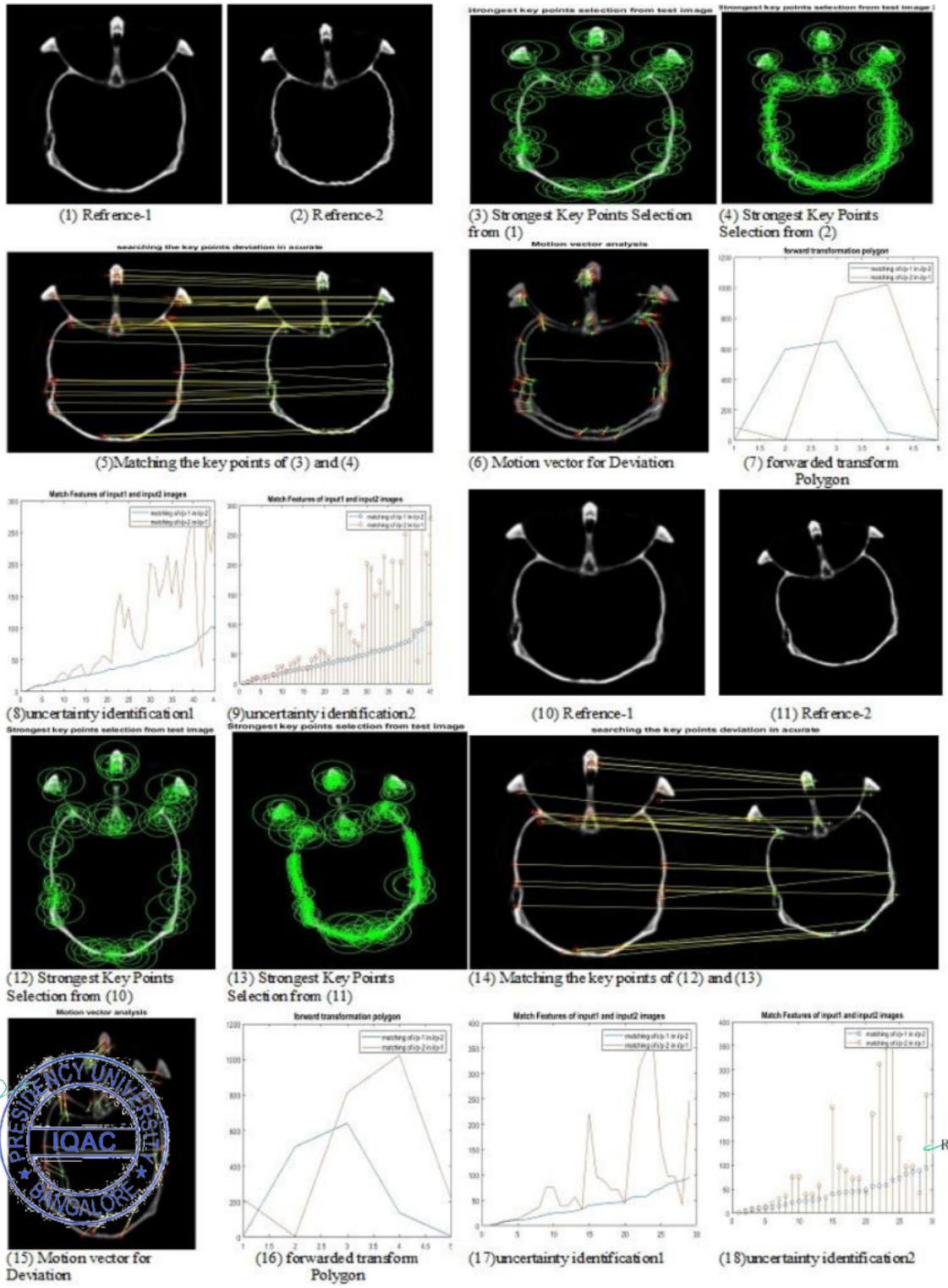

Fig 4.3: (1-9) Brain CT Scan sample after surgery with small deviation, (10- 18) Brain CT Scan sample after surgery with more deviation

Apart from registration, the proposed algorithm also verifies the features of images with respect to modalities. The above explanation holds good for the test samples in fig. 4.2 (i) and (ii). Even though the slope of the connecting line between the feature points is zero which means no deviation, but in fig. 4.2 (viii) it shows nonlinear and irregular curves, this is because the contrast of two images in fig. 4.2 (i) and (ii) is different. To avoid this confusion in the determination of deviation, fig. 4.2 (vii) will be useful. In this, forwarded transformed polygon, slope of two curves are same. In fig. 4.2 (x) and (xi) few features are not comparatively same and hence in fig. 4.2 (xvii) and (xviii) irregular spikes are observed.

The proposed algorithm also identifies the amount of deviations like "very small", "small", and "high". With the help of motion vectors, it was possible to obtain fig. 4.3 (6) and (15). During the MATLAB simulation of the test samples in fig. 4.3 (1) and (2) "very small deviation" was observed in fig. 4.3 (10) and in fig. 4.3 (11) "small deviation" was observed.

Table 4.1: Registration metrics

	Information Ratio (IR)	Lower Bound Information Ratio (LIR)	Mutual Information Ratio (MIR)	Lower Bound Mutual Information Ratio (LMIR)
Sample 1(Fig. 4.1 a and b)	114.0842	60.467	176.712	59.903
Sample 2(Fig. 4.1 j and k)	112.57	59.934	147.629	100.203
Sample 3(Fig. 4.2 i and ii)	90.54	51.531	142.009	73.409
Sample 4(Fig. 4.2 x and xi)	141.814	78.922	57.762	144.886
Sample 5(Fig. 4.3 1 and 2)	48.13	25.845	86.651	35.29
Sample 6(Fig. 4.3 10 and 11)	45.964	24.774	83.16	34.18

The Information Ratio (IR) and Mutual Information Ratio (MIR) [30] are used to analyze the performance of the proposed algorithm quantitatively. Here IR and MIR will be calculated including its lower bounds, i.e., LIR and LMIR, which are the functions of entropy and mutual information. These metrics are particularly useful to minimize the computational complexity in identifying the features count. These metrics will be useful to evaluate the registered image in the perspective of common features count that can be identified among given samples. The metrics for the six test samples of medical images are given in table 4.1.

V. CONCLUSION AND FUTURE SCOPE

This paper has focused on medical image registration and in identifying abnormalities after surgery. The existing image registration algorithms deal with feature point detection and identification, but the proposed method can also identify the quantitative analysis of registered images. The statements given above have been proved with graphical plots. In this, if there are abnormalities like loosening, subsidence and anteversion which are minor and not possible to detect by human, then the corresponding plots will show the deviation in the form of slope. That means if there is no deviation with respect to reference image, the slope becomes zero. If not, there will be a detectable slope variation. The proposed algorithm is evaluated with respect to registration metrics also. In this algorithm, we concentrated on translational movement only. There is a possibility to identify the abnormalities even if it is affected by rotational and skew motion. This will be possible through 3-D image analysis.

Conflicts of interest

The authors declare that they have no conflicts of interest regarding the publication of this article.

Data Availability

The data used to support the findings of this study are available from the corresponding authors upon request.

REFERENCES

[1] Lianghao Han, John H. Hipwell, Björn Eiben, Dean Barratt, Marc Modat, Sebastien Ourselin, David J. Hawkes *"A Nonlinear Biomechanical Model Based Registration Method for Aligning Prone and Supine MR Breast Images"* IEEE Transactions on Medical Imaging. Volume: 33, Issue: 3, 2014.

[2] Marius Staring, Keelin Murphy, Max A. Viergever, Josien P. W. Pluim "elastix: A Toolbox for Intensity-Based Medical Image Registration Stefan Klein", IEEE Transactions on Medical Imaging, Volume: 29, Issue: 1, 2010.

[3] Lianghao Han, John H. Hipwell, Björn Eiben, Dean Barratt, Marc Modat, Sebastien Ourselin, David J. Hawkes, "A Nonlinear Biomechanical Model Based Registration Method for Aligning Prone and Supine MR Breast Images", IEEE Transactions on Medical Imaging Volume: 33, Issue: 3, 2014.

[4] Aristeidis Sotiras, Christos Davatzikos, Nikos Paragios, "Deformable Medical Image Registration: A Survey" IEEE Transactions on Medical Imaging, Volume: 32, Issue: 7, 2013.

[5] Jean-Marie Guyader, Wyke Huizinga, Valerio Fortunati, Dirk H. J. Poot, Jifke F. Veenland, Margarethus M. Paulides, Wiro J. Niessen, Stefan Klein, "Group-wise Multichannel Image Registration", IEEE Journal of Biomedical and Health Informatics, Volume: 23, Issue: 3, 2019.

[6] Marzieh Golabbakhsh, Hossein Rabbani, "Vessel-based registration of fundus and optical coherence tomography projection images of retina using a quadratic registration model", IET Image Processing, Volume: 7, Issue: 8, 2013.

[7] Gorkem Saygili, Marius Staring, Emile A. Hendriks, "Confidence Estimation for Medical Image Registration Based On Stereo Confidences", IEEE Transactions on Medical Imaging, Volume: 35, Issue: 2, 2016.

[8] Dmitry V. Sorokin, Igor Peterlik, Marco Tektonidis, Karl Rohr, Pavel Matula, "Non-Rigid Contour-Based Registration of Cell Nuclei in 2-D Live Cell Microscopy Images Using a Dynamic Elasticity Model", IEEE Transactions on Medical Imaging, Volume: 37, Issue: 1, 2018.

[9] Arnaldo Mayer, Gali Zimmerman-Moreno, Ran Shadmi, Amit Batikoff, Hayit Greenspan, "A Supervised Framework for the Registration and Segmentation of White Matter Fiber Tracts", IEEE Transactions on Medical Imaging, Volume: 30, Issue: 1, 2011.

[10] Shu Liao, Albert C. S. Chung, "Non-rigid Brain MR Image Registration Using Uniform Spherical Region Descriptor", IEEE Transactions on Image Processing, Volume: 21, Issue: 1, 2012.

[11] Zhang Li, Jeroen A. W. Tielbeek, Matthan W. A. Caan, Carl A. J. Puylaert, Manon L. W. Ziech, Chung Y. Nio, Jaap Stoker, Lucas J. van Vliet, Frans M. Vos, "Expiration-Phase Template-Based Motion Correction of Free-Breathing Abdominal Dynamic Contrast Enhanced MRI", IEEE Transactions on Biomedical Engineering, Volume: 62, Issue: 4, 2015.

[12] Yangming Ou, Hamed Akbari, Michel Bilello, Xiao Da, Christos Davatzikos, "Comparative Evaluation of Registration Algorithms in Different Brain Databases With Varying Difficulty: Results and Insights", IEEE Transactions on Medical Imaging, Volume: 33, Issue: 10, 2014.

[13] Iman Aganj, Bruce Fischl, "Multimodal Image Registration Through Simultaneous Segmentation", IEEE Signal Processing, Letters Volume: 24, Issue: 11, 2017.

[14] Istvan Csapo, Brad Davis, Yundi Shi, Mar Sanchez, Martin Styner, Marc Niethammer, "Longitudinal Image Registration With Temporally-Dependent Image Similarity Measure", IEEE Transactions on Medical Imaging, Volume: 32, Issue: 10, 2013.

[15] Yuchuan Qiao, Baldur van Lew, Boudewijn P. F. Lelieveldt, Marius Staring, "Fast Automatic Step Size Estimation for Gradient Descent Optimization of Image Registration", IEEE Transactions on Medical Imaging, Volume: 35, Issue: 2, 2016.

[16] Lingjiao Pan, Liling Guan, Xinjian Chen, "Segmentation Guided Registration for 3D Spectral-Domain Optical Coherence Tomography Images", IEEE Access, Volume: 7, 2019

[17] Benjamin Hou, Bishesh Khanal, Amir Alansary, Steven McDonagh, Alice Davidson, Mary Rutherford, Jo V. Hajnal, Daniel Rueckert, Ben Glocker, Bernhard Kainz, "3-D Reconstruction in Canonical Co-Ordinate Space From Arbitrarily Oriented 2-D Images", IEEE Transactions on Medical Imaging, Volume: 37, Issue: 8, 2018.

[18] Praveen Kumar Reddy Yelampalli, Jagadish Nayak, Vilas H. Gaidhane, "Daubechies wavelet-based local feature descriptor for multimodal medical image registration", IET Image Processing, Volume: 12, Issue: 10, 2018

[19] Guha Balakrishnan, Amy Zhao, Mert R. Sabuncu, John Guttag, Adrian V. Dalca, "VoxelMorph: A Learning Framework for Deformable Medical Image Registration", IEEE Transactions on Medical Imaging, Volume: 38, Issue: 8, 2019.

[20] P. Baglietto, M. Maresca, A. Migliaro, and M. Migliardi, "Parallel implementation of the Full Search Block Matching Algorithm for Motion Estimation," in ASAP'95, pp. 182-192, IEEE Computer Society Press, July 1995.

[21] Her-Ming Jong, Liang-Gee Chen, and Tzi- Dar Chiueh, "Parallel Architectures for 3-Step Hierarchical Search Block-Matching Algorithm," IEEE Transactions on circuit and systems for video technology, Vol.4. No.4, pp.407-416, August 1994.

REGISTRAR

PRESIDENCY UNIVERSITY Registrar BANGALORE

[22] Viet L. Do and Kenneth Y. Yun *"A Low-Power VLSI Architecture for Full- Search Block-Matching Motion Estimation,"* IEEE Trans. On Circuits and System for Video Tech. Vol. 8, No. 4, pp. 393- 398, Aug. 1998.
[23] H. Yeo and Y. Hu, "A novel matching criterion and low power architecture for real-time based block based motion estimation," in Proc. ASAP'96, pp. 122-130, August 1996.
[24] R. Srinivasan and K. Rao, "Predictive coding based on efficient motion estimation," Proc. IEEE ICC'84, 1984, pp 521-526.
[25] Yanshan Li, Congzhu Yang, Li Zhang, Rongjie Xia, Leidong Fan, Weixin Xie, "A Novel SURF Based on a Unified Model of Appearance and Motion-Variation", IEEE Access, Volume: 6, 2018.
[26] Sang-Seol Lee, Sung-Joon Jang, Jungho Kim, Youngbae Hwang, Byeongho Choi, "Memory-efficient SURF architecture for ASIC implementation", Electronics Letters, Volume: 50, Issue: 15, 2014.
[27] Zhang Huijuan, Hu Qiong, "Fast image matching based-on improved SURF algorithm", 2011 International Conference on Electronics, Communications and Control (ICECC), 2011.
[28] Zhang Huiqing, Zhang Jingli, Dai Ruyong, "A fast image matching research based on MIC-SURF algorithm", The 27th Chinese Control and Decision Conference (2015 CCDC), 2015.
[29] Su Juan, Xu Qingsong, Zhu Jinghua,"A scene matching algorithm based on SURF feature" 2010 International Conference on Image Analysis and Signal Processing, 2010.
[30] Ali Khajegili Mirabadi, Stefano Rini, "The Information & Mutual Information Ratio for Counting Image Features and Their Matches", 2020 Iran Workshop on Communication and Information Theory, IWCIT 2020, ISBN 9781728182575.

G TIRUMALA VASU received the B.Tech. degree in Department of Electronics and communication Engineering from Sri Venkateswara University, Tirupati, Andhra Pradesh, India, in 2007, the M.Tech. degree in Digital Electronics and Communication Systems from Jawaharlal Nehru Technological University, Anantapuramu, Andhra Pradesh, India, in 2009. He is currently pursuing the Ph.D. degree from National Institute of Technology, Tiruchirappalli, Tamil Nadu, India and Assistant Professor in Department of Electronics and communication Engineering, Presidency University, Bangalore, Karnataka, India. His area of interest includes Image Processing and Machine Learning.

SAMREEN FIZA received the B.Tech. Degree in Electronics and Communication Engineering from Visvesvaraya Technological University (VTU), Belgaum, Karnataka, India in 2012, M.Tech. Degree in Digital Communication and Networking from Visvesvaraya Technological University (VTU), Belgaum, Karnataka, India in 2014. She is currently pursuing Ph.D. degree from Presidency University, Bangalore, Karnataka, India. At present she is working as Assistant Professor in Department of Electronics and Communication Engineering, Presidency University, Bangalore, Karnataka, India. Her area of interest includes Image Processing and Machine Learning.

G SWETHA received the B.Tech. Degree in Electronics and Communication Engineering from Jawaharlal Nehru Technological University (JNTU), Hyderabad, Telangana, India in 2005, M.Tech. Degree in VLSI Technology from Jawaharlal Nehru Technological University (JNTU), Hyderabad, Telangana, India in 2010. She is currently pursuing Ph.D. degree from Jawaharlal Nehru Technological University (JNTU), Hyderabad, Telangana, India. At present she is working as Assistant Professor in Department of Electronics and Communication Engineering, Presidency University, Bangalore, Karnataka, India. Her area of interest includes Wireless sensor networks, Image Processing and Wireless mesh networks.

HARI BANDA Received the B.Tech degree in Department of mechanical Engineering and from JNT UNIVERSITY, Anantapuramu, Andhra Pradesh, India, in 2013, the M.Tech degree in Thermal science and Energy systems in from JNT UNIVERSITY, Anantapuramu, Andhra Pradesh, India, in 2015. He is currently pursuing the Ph.D degree from National Institute of Technology, Tiruchirapalli, Tamilnadu, INDIA and Lecturer in Mechanical engineering Department, Villa College, Maldives. His area of interest includes photovoltaic cells and image processing.

PRESIDENCY UNIVERSITY IQAC BANGALORE

REGISTRAR

PRESIDENCY UNIVERSITY Registrar BANGALORE

Surgical Idiosyncrasies Credentials using Image Registration

ORIGINALITY REPORT

6%	4%	6%	%
SIMILARITY INDEX	INTERNET SOURCES	PUBLICATIONS	STUDENT PAPERS

PRIMARY SOURCES

1	Maintz, J.. "A survey of medical image registration", Medical Image Analysis, 199803 Publication	2%
2	academic.oup.com Internet Source	1%
3	"Medical Image Computing and Computer-Assisted Intervention – MICCAI 2013", Springer Nature, 2013 Publication	1%
4	arxiv.org Internet Source	<1%
5	sersc.org Internet Source	<1%
6	Sadaf Azad, Muna Al Fanah, Ci Lei. "Physical Role Limitation - It's Classification and Prediction using Machine Learning", Proceedings of the 2019 International Conference on Big Data and Education - ICBDE'19, 2019 Publication	<1%

7	"Medical Image Computing and Computer-Assisted Intervention – MICCAI 2009", Springer Science and Business Media LLC, 2009 Publication	<1 %
8	Zhao, Y.. "The Cyclicity of the Period Annulus of the Quadratic Hamiltonian Systems with Non-Morsean Point", Journal of Differential Equations, 20000320 Publication	<1 %
9	ijeert.org Internet Source	<1 %
10	hdl.handle.net Internet Source	<1 %
11	"Biomedical Image Registration", Springer Science and Business Media LLC, 2014 Publication	<1 %
12	"Machine Learning in Medical Imaging", Springer Science and Business Media LLC, 2020 Publication	<1 %
13	Bina Bhandari, R. H. Goudar, Kaushal Kumar. "Quine-McCluskey: A Novel Concept for Mining the Frequency Patterns from Web Data", International Journal of Education and Management Engineering, 2018 Publication	<1 %

14	"Medical Image Computing and Computer Assisted Intervention – MICCAI 2017", Springer Science and Business Media LLC, 2017 Publication	<1%
15	"Motion Estimation for Video Coding", 'Springer Science and Business Media LLC', 2015 Internet Source	<1%

Exclude quotes	Off	Exclude matches	Off
Exclude bibliography	On		

PRESIDENCY UNIVERSITY BANGALORE IQAC

REGISTRAR

PRESIDENCY UNIVERSITY BANGALORE Registrar